Bioresource Technology 130 (2013) 463–471

Contents lists available at SciVerse ScienceDirect

Bioresource Technology

journal homepage: www.elsevier.com/locate/biortech

Characteristics and nutrient values of biochars produced from giant reed at different temperatures

Hao Zheng [a,b], Zhenyu Wang [a,*], Xia Deng [a], Jian Zhao [b], Ye Luo [a], Jeff Novak [c], Stephen Herbert [b], Baoshan Xing [b,*]

[a] College of Environmental Science and Engineering, Ocean University of China, Qingdao 266100, China
[b] Stockbridge School of Agriculture, University of Massachusetts, Amherst, MA 01003, USA
[c] USDA-ARS Coastal Plain Soil, Water & Plant Research Center, 2611 W. Lucas Street, Florence, SC 29501, USA

HIGHLIGHTS

- Available N and P in biochar decreased with increasing temperature but K increased.
- Less-soluble crystalline P minerals were formed in high-temperature biochar.
- More NH_4^+, PO_4^{3-} and K^+ were released from the biochars at low pH ($\leqslant$5).
- Biochars released NH_4^+ slowly but released PO_4^{3-} and K^+ fast.
- Low-temperature biochars could be a good amendment for improving soil fertility.

ARTICLE INFO

Article history:
Received 9 April 2012
Received in revised form 7 December 2012
Accepted 8 December 2012
Available online 17 December 2012

Keywords:
Biochar
Pyrolysis temperature
Giant reed
Nutrient values
Adsorption

ABSTRACT

To investigate the effect of pyrolysis temperature on properties and nutrient values, biochars were produced from giant reed (*Arundo donax* L.) at 300–600 °C and their properties such as elemental and mineral compositions, release of N, P and K, and adsorption of N and P were determined. With increasing temperatures, more N was lost and residual N was transformed into heterocyclic-N, whereas no P and K losses were observed. P was transformed to less soluble minerals, resulting in a reduction in available-P in high-temperature biochars. A pH of $\leqslant$ 5 favored release of NH_4^+, PO_4^{3-} and K^+ into water. Low-temperature biochars ($\leqslant$ 400 °C) showed appreciable NH_4^+ adsorption (2102 mg kg^{-1}). These results indicate that low-temperatures may be optimal for producing biochar from giant reed to improve the nutrient availability.

1. Introduction

Biochar refers to the carbon-rich product from heating biomass in a closed system under limited oxygen supply. It is distinguished from charcoal by its use as a soil amendment (Lehmann and Joseph, 2009). It is a multifunctional material with environmental and agricultural applications (Atkinson et al., 2010; Beesley et al., 2011). Biochar is recognized as a high-efficient and low-cost sorbent for pollutants (Silber et al., 2010; Sun et al., 2011; Wang and Xing, 2007). Application of biochar to soil has been proposed as an approach to sequester carbon (Lehmann and Joseph, 2009) and to possibly reduce or suppress CO_2, CH_4 and N_2O emissions (Spokas et al., 2009). Most importantly, biochar may improve soil quality and nutrient availability to plants (Atkinson et al., 2010). Although information on biochar nutrient properties are available (Atkinson et al., 2010; Chan et al., 2009; Lehmann and Joseph, 2009; Silber et al., 2010), the mechanism of nutrient release from biochar is not fully understood. Furthermore, total N, P and K (TN, TP and TK) in biochars may not necessarily reflect the actual availability of these nutrients to plants (Spokas et al., 2012). The influence of pyrolysis temperature on the production of biochars that are suitable as soil fertilizer still needs to be elucidated. Although it has been shown that NO_3^- and NH_4^+ leaching was reduced from soils amended with biochars (Novak et al., 2010), the influence of time and pH on nutrient release from biochars produced at different temperatures remains to be explored.

Giant reed (*Arundo donax* L.) (GR), a perennial grass, is widespread in many aquatic ecosystems in China (Yan et al., 2005). Due to its fast growth rate and good resistance to drought and floods, GR may yield up to 45 tons per hectare and life cycle

* Corresponding authors. Tel.: +1 413 545 5212 (B. Xing).
E-mail addresses: wang0628@ouc.edu.cn (Z.Y. Wang), bx@umass.edu (B.S. Xing).

0960-8524/$ - see front matter © 2012 Elsevier Ltd. All rights reserved.
http://dx.doi.org/10.1016/j.biortech.2012.12.044

assessments indicate that it could be a suitable feedstock for biochar production (Roberts et al., 2010).

Biochars were prepared from GR at different temperatures using oxygen-limited pyrolysis. The aims of the present study were to (1) investigate the influence of pyrolysis temperature on nutrient composition of biochars and the mechanisms of nutrient release from biochars; (2) evaluate the influence of time and pH on the release of plant-available nutrients from biochars alone; and (3) examine the sorption behavior of NH_4^+, NO_3^- and PO_4^{3-} onto biochars.

2. Methods

2.1. Production of biochars

Two batches of biochar were produced at 300, 350, 400, 500 or 600 °C for 2 h from GR stems (1.0 kg) without leaves using a vacuum tube furnace (O-KTF1200, China) under a N_2 flow of 500 mL min^{-1}. The pyrolysis temperature was raised to the desired values at a ramp rate of 10 °C min^{-1}. Biochar yields were recorded and the samples were milled to pass a 0.12 mm (120 mesh), and the biochars produced at the same temperature were mixed and homogenized for further analysis. The biochars are hereafter referred to as BC300, BC350, BC400, BC500 and BC600, respectively. BC0 is the raw material. Ash (BCA) was produced by placing the raw material into a ceramic crucible and heated at 750 °C for 4 h under air.

2.2. Characterization of samples

Total C, N, H, and O were determined in duplicate with an elemental analyzer (MicroCube, Elementar, Germany). Brunauer–Emmett–Teller (BET) surface areas (S_{BET}) were obtained from N_2 adsorption at 77 K using Quantachrome Autosorb-1 (Autosorb-1, Quantachrome, USA). Ash contents of biochars were measured by the production of BCA. The pH values of all samples were measured at a ratio of 1:20 (w/v) in water after being shaken for 24 h at 130 rpm. X-ray diffraction (XRD) patterns were obtained using a Macscience-M18XHF instrument (UK) with Cu Kα radiation at 40 mA and 40 kV. Scanning electron microscopy (SEM) imaging analysis was conducted using a HITACHI S-4800 Scanning Microscope. Zeta potentials were measured by a zeta potential analyzer (90Plus, Brookhaven, USA) (Yuan et al., 2011). The total acidic oxygen-containing groups of the biochar samples were determined using Boehm's titration method (Boehm, 1994).

2.3. Nutrient content in biochars

Water-soluble mineral elements released from biochars were determined in a background electrolyte solution with 0.01 M NaCl (Silber et al., 2010) to maintain a constant ionic strength and 200 mg L^{-1} NaN_3 to inhibit microbial activity. A biochar sample (1.0 g) was placed in a 40-mL glass vial and 36 mL of background electrolyte solution was added. After being shaken at 130 rpm for 72 h at room temperature (22 ± 1 °C), the suspension was centrifuged at 1742 g for 30 min. PO_4^{3-}, NH_4^+ and NO_3^- in the supernatant were determined using a Flow Injector Autoanalyzer (QuickChem 8500, Lachat, USA) and K^+ was measured with an ion chromatograph (ICS-3000, Dionex, USA). Acid-soluble and KCl-extractable NH_4^+, NO_3^-, and PO_4^{3-} were determined in 0.5 M HCl and 1 M KCl solutions, respectively, and acid-soluble K^+ was also measured using the ion chromatograph. TP in biochars was measured after dry-ashing using a colorimetric method (Page et al., 1982). For determination of TK, biochar was digested in concentrated acid (0.15 g samples in 10 mL 70% HNO_3 at 120 °C for 24 h) and K concentration was quantified using ICP (Silber et al., 2010).

2.4. Effect of time and pH on water-soluble nutrients release

A biochar sample (1.0 g) was placed in a 40-mL glass vial and 36 mL of background electrolyte solution (see Section 2.3) was added. After being shaken at 130 rpm, 30-mL supernatants were removed using a glass pipette without any biochar loss and the vials were refilled with the same amount of background solution and re-extracted at 2, 6, 12, 24, 48, 72, 96, 120, 144 and 168 h. Each sample was run in triplicate. The concentration of NH_4^+, NO_3^-, PO_4^{3-} and K^+ were determined as described in Section 2.3. Triplicate samples with no biochars were concurrently run as controls.

The effect of pH on water-soluble NH_4^+, NO_3^-, PO_4^{3-} and K^+ released from biochars was studied in background electrolyte solution adjusted to pHs from 2 to 12. The suspension pH was adjusted to the predetermined values and kept constant throughout the experiment by adding small volumes of 0.1–1.0 M HCl or NaOH. After being shaken at 130 rpm for 72 h, the concentrations of NH_4^+, NO_3^-, PO_4^{3-} and K^+ in supernatants were determined as described in Section 2.3. Each sample was run in duplicate. Duplicate samples with no biochars were concurrently run as controls.

2.5. NH_4^+ and NO_3^- sorption

Sorption isotherms were obtained using a batch equilibration technique. Appropriate amounts of samples were placed into vials so that the solid/solution ratio would result in 20–80% uptake of NH_4^+ and NO_3^-. The solid/solution ratios for sorption of NH_4^+ by BC300 and BC350 were 0.35 g/12 mL and 0.8 g/12 mL for BC400, BC500 and BC600. A ratio of 0.3 g/8 mL was used for sorption of NO_3^- by all biochars. The test solutions of 0–200 mg L^{-1} NH_4^+—N and 0–100 mg L^{-1} NO_3^-—N were prepared from stock solutions of 1000 mg L^{-1} NH_4^+—N prepared from NH_4Cl and 1000 mg L^{-1} NO_3^-—N prepared from $NaNO_3$ in background solutions containing 0.01 M KCl and 200 mg NaN_3. During the shaking period of 72 h, the pH of suspension was maintained at 7.0 ± 0.1 by adding small volumes of 0.1–1.0 M HCl or NaOH. The samples were centrifuged at 1742 g for 30 min and the concentrations of NH_4^+ and NO_3^- in supernatants were determined as described in Section 2.3. All samples were run in duplicate along with blanks. Because the mass loss of solute was negligible, sorption of solutes by biochars was determined by mass balance.

2.6. Data analysis

The nutrient release results were examined for NH_4^+, PO_4^{3-} and K^+ solubilized from biochars using pseudo-first-order (Kasozi et al., 2010), pseudo-second order (Kasozi et al., 2010) and power models (Sparks, 2003), which can be presented as

$$\ln(q_e - q_t) = \ln q_e - k_1 t \quad (1)$$

$$t/q_t = 1/k_2 q_e^2 + t/q_e \quad (2)$$

$$q_t = at^b \quad (3)$$

respectively, where q_e and q_t (mg kg^{-1}) are the release capacities at equilibrium and at time t, respectively; k_1 (h^{-1}) is the rate constant of pseudo-first order release, k_2 (h^{-1}) is the rate constant of pseudo-second order release, a ((mg kg^{-1} h^{-1})^b) and b ((mg kg^{-1})$^{-1}$) are constants that relate to the initial concentration of nutrients released and the rate of change in nutrients release over time, respectively.

With respect to sorption, nonlinear Freundlich and Langmuir models were used to fit the NH_4^+ and NO_3^- sorption isotherm data:

$$Q_e = K_F C_e^n \quad (4)$$

$$Q_e = Q^0 C_e/(K_L + C_e) \quad (5)$$

where Q_e (mg kg^{-1}) and C_e (mg L^{-1}) are the equilibrium solid and aqueous concentrations, respectively; K_F ((mg kg^{-1})/(mg L^{-1})^n) and K_L (mg L^{-1}) are Freundlich and Langmuir affinity coefficients, respectively; n is the Freundlich exponential coefficient; Q^0 (mg kg^{-1}) is the maximum sorption capacity of solute.

Results are expressed as the average of three replicates with standard deviation. Significant differences of nutrients among the temperatures were tested using Duncan's multiple range test ($P = 0.05$) and the correlation was analyzed with the Pearson test (two-tailed) at $P = 0.01$ or 0.05 by means of Statistical Product and Service Solutions Software (SPSS, version 18.0).

3. Results and discussion

3.1. Characteristics of biochars

The mass yield of biochar decreased with increasing pyrolysis temperature from 44.4% of the original feedstock mass at 300 °C to 30.6% at 600 °C (Table 1, Supplementary Fig. S1). The amount of inorganic constituents remaining in the biochars during pyrolysis increased with increasing temperature, consistent with the higher ash contents (Table 1). The temperature trend for the ash content was similar to that of other organic waste such as pine needle (Chen et al., 2008) and manure (Cantrell et al., 2012), but the ash content in the biochars was much lower than that produced from corn and canola straw (Yuan et al., 2011). The pH of the biochars (Table 1) also exhibited a significant positive linear correlation with pyrolysis temperature ($r = 0.916$, $P < 0.05$, Fig. S1). The pH values and ash contents were positively correlated ($r = 0.981$, $P < 0.01$, Fig. S2), hence, the minerals were probably the main cause of each biochar' s inherent alkaline pH. The higher pH for BC500 and BC600 indicates their potential use as amendments to reduce soil acidity.

The C content in the biochars increased with increasing pyrolysis temperature (except for BCA), whereas the O and H contents decreased (Table 1). The H/C and O/C atomic ratios also decreased with increasing pyrolytic temperatures (van Krevelen diagram, Fig. S3). These data reflected the increasing degree of structural modification due to carbonization reactions of biochar with increasing temperature. For example, high-temperature biochars (BC500 and BC600) were highly carbonized and exhibited a high degree of carbon in aromatic structures (Novak et al., 2009; Keiluweit et al., 2010). The surface areas (S_{BET}) (Table 1) of biochars below 500 °C were extremely low (2.16–3.04 $m^2\ g^{-1}$), while the S_{BET} of BC600 was far higher at 50 $m^2\ g^{-1}$. All the biochars have a typical plant cell structure, and the differences between BC300, BC350, BC400 and BC500 in the SEM micrographs were negligible, but the pore volumes in BC600 were higher (Fig. S4), which is consistent with the result of S_{BET}. No pore structure was found in BCA (Fig. S4), due to removal of the bulk of the carbon structure and fusion or sintering of inorganic materials. The total amount of acidic oxygen-containing functional groups on the surface of biochars was negatively correlated with the pyrolytic temperature (Fig. S1), consistent with the decrease in the polarity index [(N + O)/C] (Table 1). Based on the pH-zeta potential plot (Fig. S5), the point of zero net charge (PZNC) of the biochar samples was around pH 2, as also seen in other studies (Silber et al., 2010; Yuan et al., 2011). Surface charges on each biochar were negative at pH 7 (Fig. S6), caused by deprotonation of the oxygen-containing functional groups such as carboxyl and hydroxyl groups (Novak et al., 2009). The negative charge on the surface of these biochars decreased with increasing temperatures (Fig. S6) due to loss of oxygen-containing functional groups (Chen et al., 2008).

When BC600 was ashed with air at 550 °C for 1 and 2 h in a muffle furnace to reduce the carbon content, BC600-1 and BC600-2 were obtained, respectively. The XRD spectra of these samples are shown in Fig. S7. Sharp peaks in all samples indicate the presence of miscellaneous inorganic components, whereas no sharp peaks were observed in the spectra for BC0, indicating that no crystalline minerals existed in raw giant reed (Keiluweit et al., 2010). Sylvine (KCl) was present in all samples, reflected by peaks at 0.315, 0.222, 0.182, 0.141 and 0.128 nm (Silber et al., 2010). Peak intensities increased with increasing temperature, indicating that sylvine was well crystallized in high-temperature biochars. The peaks at 0.301, 0.257 and 0.208 nm were only present in five biochar samples and were assigned to dolomite ($CaMg(CO_3)_2$) (Yuan et al., 2011). The peaks at the same position in BC600-1, BC600-2 and BCA were assigned to larnite (Ca_2SiO_4) and enstatite ($Mg_2Si_2O_6$) (Etiégni and Campbell, 1991), suggesting that loss of carbonate and formation of crystallized silicate increased with the increasing temperatures. In addition, wollastonite ($CaSiO_3$) was found in BC600-1, BC600-2 and BCA at 0.388 nm (Wang et al., 2001), which further showed that more crystalline silicate minerals associated with Ca and Mg were formed in high-temperature biochars (BC600). Potassium dihydrogen phosphate (KH_2PO_4) and magnesium cyclo-tetraphosphate ($Mg_2P_4O_{12}$) were observed at 0.301 nm in BC300, BC350 and BC400 while only $Mg_2P_4O_{12}$ was present in BC500 and BC600. Interestingly, magnesium diphosphate ($Mg_2P_2O_7$) was found not only at 0.301 nm but also at 0.447 and 0.293 nm, and the peak was sharper in BC600-1, BC600-2 and BCA than BC600, indicating $Mg_2P_4O_{12}$ further crystallized to $Mg_2P_2O_7$. Therefore, phosphate minerals in biochars

Table 1
Physical and chemical properties of biochars.

Sample	Yield/%	Component[β], wt.%							Atomic ratio				pH[γ]	SAGs[δ] mmol g^{-1}	S_{BET} $m^2\ g^{-1}$
		C	H	O	N	P	K	Ash	C:N	O:C	H:C	(O + N)/C			
BC0[α]	100.0	45.38	5.75	43.86	0.32	0.05	1.48	3.66	164	0.73	1.51	0.73	5.68a	NA[ε]	1.69
BC300	44.4	65.26	4.51	21.03	0.65	0.12	3.70	7.69	117	0.24	0.82	0.25	8.42c	2.69	2.72
BC350	41.7	66.97	4.46	21.67	0.64	0.12	3.80	7.73	121	0.24	0.79	0.25	8.09b	2.27	2.16
BC400	40.0	72.25	4.09	18.72	0.69	0.13	4.18	8.45	121	0.19	0.67	0.20	8.06b	1.75	3.04
BC500	33.4	73.12	3.01	11.54	0.63	0.16	4.77	10.70	136	0.12	0.49	0.13	9.73d	1.16	2.58
BC600	30.6	78.61	2.22	11.24	0.55	0.17	5.02	11.27	165	0.11	0.34	0.11	10.67e	0.98	50
BCA	NA	2.74	1.25	25.22	0.04	1.50	37.64	95.61	79.	6.92	5.45	6.93	11.62f	NA	4.50

[α] BC0 represents raw giant reed; BC300 through BC600 represent the biochars produced at 300–600 °C; BCA represents the ash sample.
[β] Yields and ash contents are on a water-free basis (dried at 105 °C). Elemental contents and atomic ratios are on water and ash-free basis.
[γ] The different small letter behind the number means significant difference at $P = 0.05$, $n = 3$. The different small letter behind the pH value indicated significant difference, which was adopted Duncan's multiple range test ($P = 0.05$).
[δ] SAGs: surface acid function groups.
[ε] NA: data were not obtained.

became more crystallized with increasing temperature, which is supported by the results of formation of crystallized phosphate associated with Ca and Mg in dairy-manure-derived biochar (Cao and Harris, 2010).

3.2. N, P and K in biochars

TN contents were relatively stable in all biochars (Table 1), although more N was lost with increasing temperature (Fig. S8). Similarly, Lang et al. (2005) reported that N losses began at ~400 °C and at least half of the N was lost as volatiles at ~750 °C in three woody and four herbaceous biochars. Since N is associated with many organic molecules, N begins to volatilize at relatively low temperatures (~200 °C) (DeLuca et al., 2009). The loss of TN in the biochars was attributed to the removal of N via volatilization (Cao and Harris, 2010; Lang et al., 2005).

The contents of water-soluble NH_4^+ (W-NH_4^+) increased from 20.4 mg kg^{-1} in BC300 to 34.4 mg kg^{-1} in BC350, then decreased to 8.0 and 5.7 mg kg^{-1} in BC500 and BC600, respectively (Fig. 1a). The contents of KCl-exchangeable NH_4^+ (KCl-NH_4^+) also had this temperature-dependent pattern (Fig. 1a). The contents of water-soluble and KCl-exchangeable NO_3^- (W-NO_3^- and KCl-NO_3^-) in the biochars were 2.3–5.2 mg kg^{-1} and 2.0–5.8 mg kg^{-1}, respectively, and decreased with increasing pyrolysis temperature (Fig. 1b). The content of available NH_4^+ in BC350 (65.5 mg kg^{-1}) was much higher than that produced from ponderosa pine (2.2 mg kg^{-1}) (Gundale and DeLuca, 2006) and manure (below detection limits) (Cantrell et al., 2012).

The decrease in available N in higher temperatures biochars was attributed to the loss of TN and heterocyclizaiton of N during pyrolysis (Koutcheiko et al., 2007). In addition, the relatively stable content of HCl-extracted NH_4^+ (10.31–14.69 mg kg^{-1}, Fig. 1a) exclude that formation of N minerals in biochars was not the main reason for more available N reductions in the high temperature biochars. Minerals associated with N were not found in the XRD spectra (Fig. S7) and those reported previously (Keiluweit et al., 2010; Silber et al., 2010).

Unlike TN contents in biochars, TP content significantly increased with temperature ($P = 0.05$) from 0.05% in BC0 to 0.12% in BC300, and 0.17% in BC600 (Table 1, Fig. 1c and Fig. S9). The

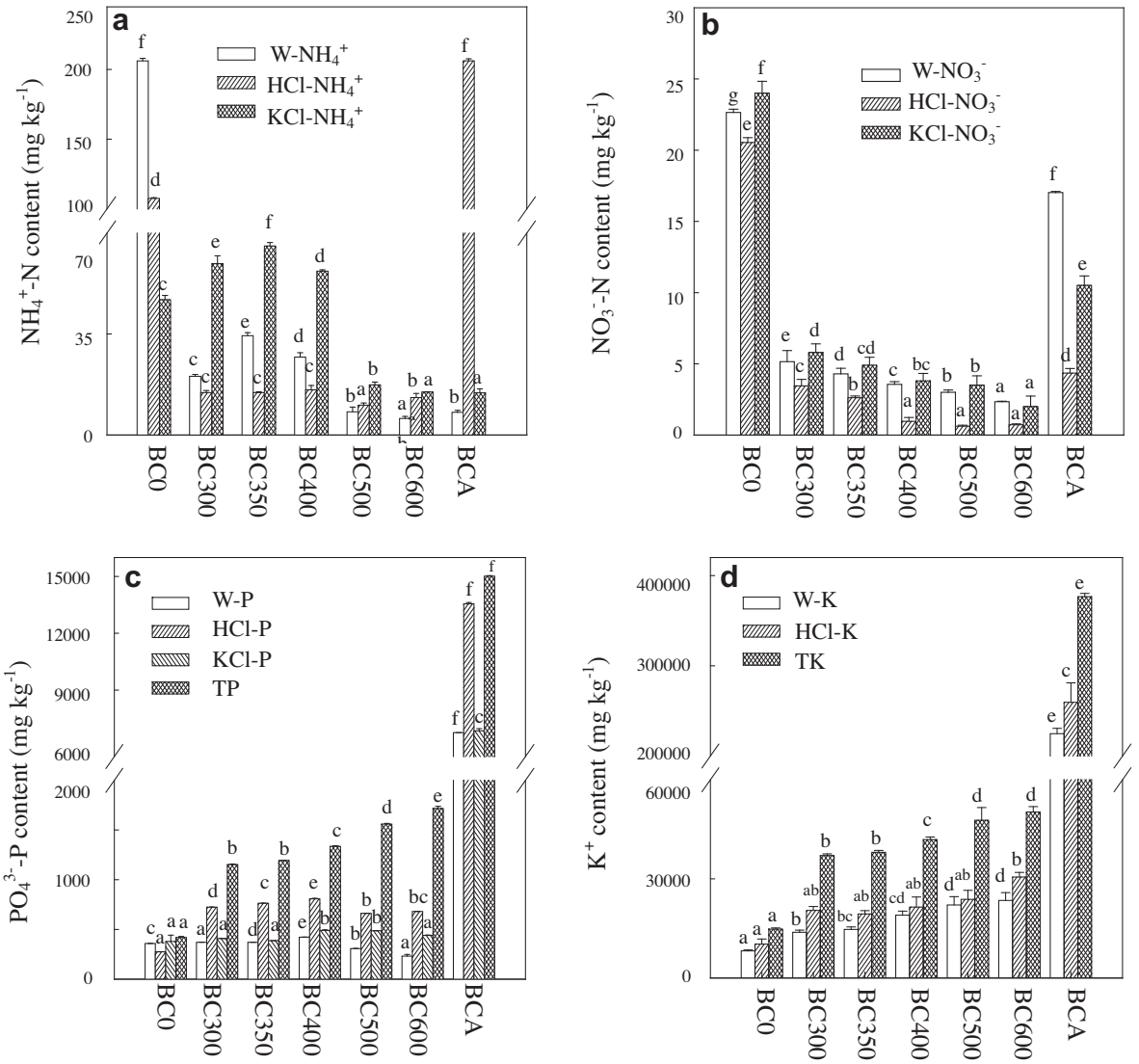

Fig. 1. The content of N, P and K extracted by different solutions from biochars: (a) NH_4^+; (b) NO_3^-; (c) PO_4^{3-}; (d) K^+. The different letters among different biochars indicate significant difference, which was analyzed by Duncan's multiple range test ($P = 0.05$). BC0 represents raw giant reed; BC300 through BC600 represent the biochars produced at 300–600 °C; BCA represents the ash sample.

TP increase in the biochars with increasing temperature was ascribed to the loss of carbon, and relatively stable P in plant biomass in response to heating (Page et al., 1982). No P was lost, confirming that P forms were stable during pyrolysis. Bridle and Pritchard (2004) also found a 100% recovery of P in a biochar prepared at 450 °C.

The water-soluble PO_4^{3-} (W-P) concentration did increase initially from 359 mg kg^{-1} (85.7% of TP) in BC0 to ~370 mg kg^{-1} (32.2% of TP) in BC300 and BC350, to 422 mg kg^{-1} (31.6% of TP) in BC400, then decreased to 308 mg kg^{-1} (19.7% of TP) in BC500 and 232 mg kg^{-1} (13.51% of TP) in BC600 (Fig. 1c). The KCl-exchangeable PO_4^{3-} (KCl-P) concentration had a similar trend and the amount was 35.4% and 25.6% of TP in BC300 and BC600, respectively (Fig. 1c). The TP contents (0.12–0.17%) in the biochars were similar to that of green waste compost (0.16–0.38%) (Chan et al., 2009). Actually, the available P (387–491 mg kg^{-1}) in the biochars was much higher than that produced from Douglas-fir (12–56 mg kg^{-1}) (Gundale and DeLuca, 2006) and similar to that produced from high P content manure (380–460 mg kg^{-1}) (Cantrell et al., 2012). Thus, the low-temperature biochars (⩽400 °C) also may be a good amendment to bolster P concentrations in P-deficient soils.

The available P increase in the low-temperature biochars (⩽400 °C) could be explained by the reduction of biomass via carbon loss (Table 1) and the presence of less crystallized P-associated minerals (Fig. S7). With increasing temperature, increasing crystallized minerals formed to associate with P, creating less-soluble P forms (Figs. S7 and S10). The content of HCl-extracted P (HCl-P) in the biochars showed a similar temperature-dependent trend as that of W-P; however, the content of HCl-P was almost twice that of W-P in BC300, BC350, BC400 and BC500 and three times that of BC600 (Fig. 1c). The content of HCl-P was 60.5–63.9% of TP in BC300, BC350 and BC400, 39.6–42.4% of TP in BC500 and BC600 (Fig. 1c). These data demonstrated that the more P-crystallized minerals (less water soluble) formed in these biochars. Also, the content of water-soluble Ca and Mg significantly decreased in BC500 and BC600 (Fig. S11). These findings, as supported by the XRD results (Fig. S7), confirmed that the soluble P in low-temperature biochars (⩽400 °C) was converted to less-soluble minerals associated with Ca and Mg in the high-temperature pyrolyzed biochars (⩾500 °C).

The TK content increased with increasing temperature (Fig. 1d, Fig. S9). The TK content significantly ($P = 0.05$) increased from 3.70% in BC300 to 5.02% in BC600. No K was lost during pyrolysis in the present study, whereas Yu et al. (2005) reported that 48% of TK was lost between 473 and 673 °C during pyrolysis of rice straw. Additionally, K volatilization began between 700 and 800 °C during production of wood-based biochar (DeLuca et al., 2009). Thus, 600 °C is an ideal temperature to retain more K in GR-derived biochars. The available K (water-soluble K, W-K, Fig. 1d) content significantly ($P = 0.05$) increased with increasing pyrolysis temperature (37% and 47% of TK in BC300 and BC600, respectively). Thus, with increasing temperature, a greater proportion of the TK pool was in an available form. The W-K content in the biochars was less than half of the TK content, and most of the K in the biochars was transformed into crystallized minerals under pyrolysis. This finding is supported by the content of acid-soluble K (HCl-K) (Fig. 1d) and XRD data (Fig. S7). It has been reported that K was well dispersed in the biochar matrices and may be bound to O in biochars as ionic phenoxides (Wornat et al., 1995). The TK content in common organic fertilizers (e.g. poultry manure) was reported to be between 0.1% and 1.6% (Chan et al., 2009), which was much lower than that of the present biochars (3.70–5.02%) and similar to their available K contents (1.38–2.35%). Thus, high-temperature biochars (e.g., BC600) could be a suitable amendment for K-deficient soils.

3.3. Kinetics of N, P and K release from biochars

The results of N, P and K release kinetics experiments of biochars are shown in Fig. 2. The NH_4^+ release from biochars mainly occurred within 120 h, followed by a slow increase (less than 15%) from 120 to 168 h (Fig. S12a), indicating that these biochars contain slow-release NH_4^+. In contrast, the PO_4^{3-} and K^+ release (>85%) mainly occurred within 24 h (Fig. S12b and c), showing that these biochars contained fast-release PO_4^{3-} and K^+. When used in a greenhouse or field situation, the PO_4^{3-} and K^+ forms supplied by this biochar would be readily available for plant uptake. Thus, these biochars could be useful to augment crop fertilizer needs.

The nutrient release kinetic data were fitted using three kinetic models to better understand the processes governing NH_4^+, PO_4^{3-} and K^+ release from biochars (Table 2). The calculated q_e (q_e/cal)

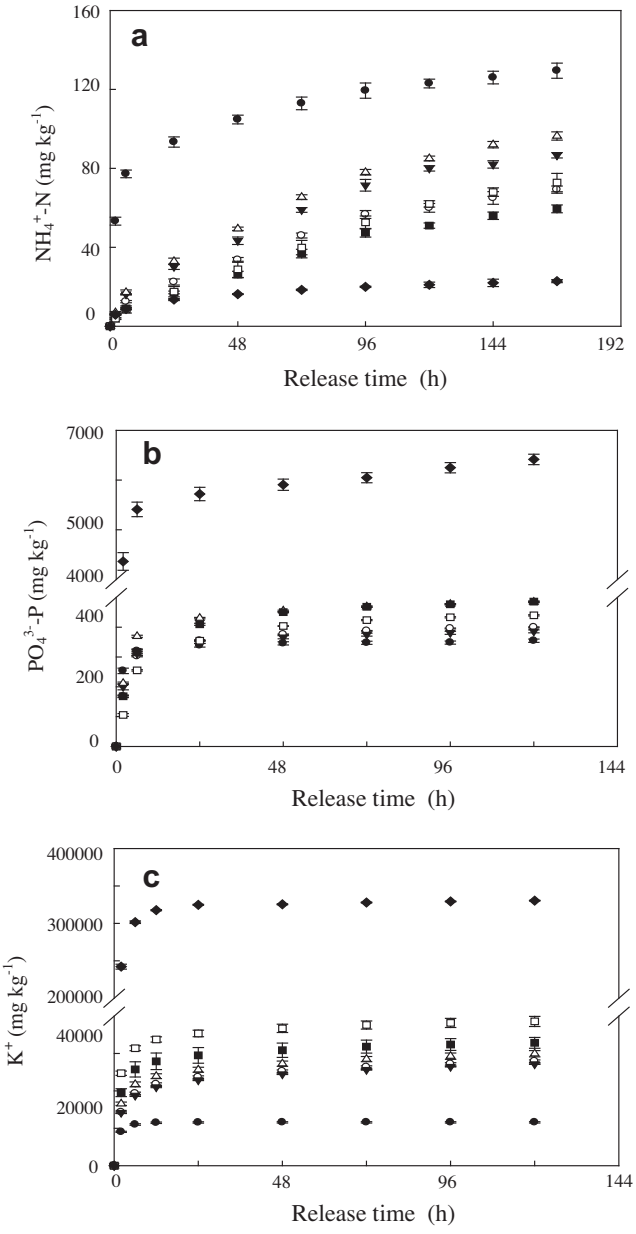

Fig. 2. Release kinetics of water-soluble PO_4^{3-}, NH_4^+ and K^+ from biochars: (a) PO_4^{3-}; (b) NH_4^+; (c) K^+. Symbols stand for BC0 (●), BC300 (○), BC350 (▼), BC400 (△), BC500 (■), BC600 (□) and BCA (♦). BC0 represents raw giant reed; BC300 through BC600 represent the biochars produced at 300–600 °C; BCA represents the ash sample.

Table 2
Estimated kinetic model parameters for nutrients released from biochars.

Nutrient	Biochar	q_e/exp[β]	Pseudo-first-order			Pseudo-second order			Power		
			$k_1 \times 10^2$	q_e/cal	R^2	$k_2 \times 10^3$	q_e/cal	R^2	a	b	R^2
NH_4^+	BC0[α]	129.5	2.15 ± 0.16	78.1 ± 1.13	0.9627	0. 95 ± 0.40	132 ± 4.90	0.9963	52.3 ± 1.97	0.18 ± 0.01	0.9955
	BC300	69.23	1.80 ± 0.11	71.4 ± 1.08	0.9806	0. 23 ± 0.06	86.2 ± 11.7	0.9385	4.28 ± 0.56	0.55 ± 0.03	0.9942
	BC350	86.64	2.00 ± 0.10	91.4 ± 1.09	0.9779	0. 19 ± 0.04	109 ± 13.5	0.9526	5.83 ± 0.85	0.54 ± 0.03	0.9923
	BC400	96.40	1.94 ± 0.13	101 ± 1.10	0.9711	0. 16 ± 0.03	120 ± 12.4	0.9586	6.34 ± 0.68	0.54 ± 0.02	0.9959
	BC500	59.51	1.79 ± 0.13	64.2 ± 1.10	0.9608	0. 19 ± 0.05	79.4 ± 13.6	0.9079	2.65 ± 0.41	0.61 ± 0.03	0.9939
	BC600	72.83	1.70 ± 0.15	81.7 ± 1.13	0.9373	0.10 ± 0.02	107 ± 25.2	0.8387	1.95 ± 0.29	0.71 ± 0.03	0.9958
	BCA	22.87	2.00 ± 0.10	18.0 ± 1.08	0.9836	2.71 ± 0.93	24.0 ± 1.31	0.9904	5.25 ± 0.17	0.29 ± 0.01	0.9985
PO_4^{3-}	BC0	354.6	3.39 ± 0.99	84.9 ± 1.64	0.6999	2.80 ± 1.62	357 ± 2.81	0.9998	265 ± 13.3	0.06 ± 0.01	0.9864
	BC300	399.7	4.18 ± 0.50	204 ± 1.28	0.9338	8.02 ± 0.19	400 ± 4.00	0.9997	199 ± 23.7	0.15 ± 0.03	0.9590
	BC350	386.1	3.87 ± 0.61	163 ± 1.35	0.8895	1.11 ± 0.34	385 ± 3.76	0.9998	223 ± 20.2	0.12 ± 0.02	0.9698
	BC400	484.4	3.87 ± 0.53	235 ± 1.30	0.9140	0.68 ± 0.17	500 ± 5.53	0.9997	247 ± 27.7	0.14 ± 0.03	0.9619
	BC500	485.7	3.89 ± 0.40	287 ± 1.22	0.9504	0.45 ± 0.07	500 ± 5.43	0.9997	201 ± 25.2	0.19 ± 0.03	0.9650
	BC600	439.8	4.14 ± 0.29	307 ± 1.15	0.9767	0.35 ± 0.04	455 ± 4.88	0.9997	146 ± 24.8	0.24 ± 0.04	0.9557
	BCA	6415	2.80 ± 0.65	2261 ± 1.38	0.7859	0.13 ± 0.09	5000 ± 91	0.9987	4404 ± 164	0.07 ± 0.01	0.9930
K^+	BC0	11590	22.6 ± 4.85	4274 ± 182	0.8788	0.30 ± 0.14	11628 ± 22	1.0000	9712 ± 453	0.04 ± 0.01	0.9827
	BC300	27926	3.13 ± 0.42	13137 ± 122	0.9024	0.011 ± 0.006	28314 ± 558	0.9988	14612 ± 670	0.14 ± 0.01	0.9902
	BC350	27152.71	3.15 ± 0.41	12923 ± 111	0.9091	0.013 ± 0.007	27548 ± 566	0.9987	14251 ± 559	0.14 ± 0.01	0.9928
	BC400	29938.39	3.23 ± 0.44	13255 ± 123	0.8984	0.010 ± 0.004	30317 ± 553	0.9990	16787 ± 662	0.12 ± 0.01	0.9920
	BC500	32846.50	3.64 ± 0.54	12483 ± 128	0.8849	0.013 ± 0.004	33205 ± 365	0.9996	20409 ± 969	0.10 ± 0.01	0.9871
	BC600	38570.06	3.81 ± 0.60	13076 ± 132	0.8724	0.014 ± 0.004	38923 ± 335	0.9998	25687 ± 1090	0.09 ± 0.01	0.9887
	BCA	330354.80	4.60 ± 1.07	57826 ± 165	0.7543	0.005 ± 0.001	331664 ± 692	1.0000	259961 ± 12840	0.06 ± 0.01	0.9818

[α] BC0 represents raw giant reed; BC300 through BC600 represent the biochars produced at 300–600 °C; BCA represents the ash sample.
[β] The unit of *qe/exp* and *qe/cal* is mg kg^{-1}.

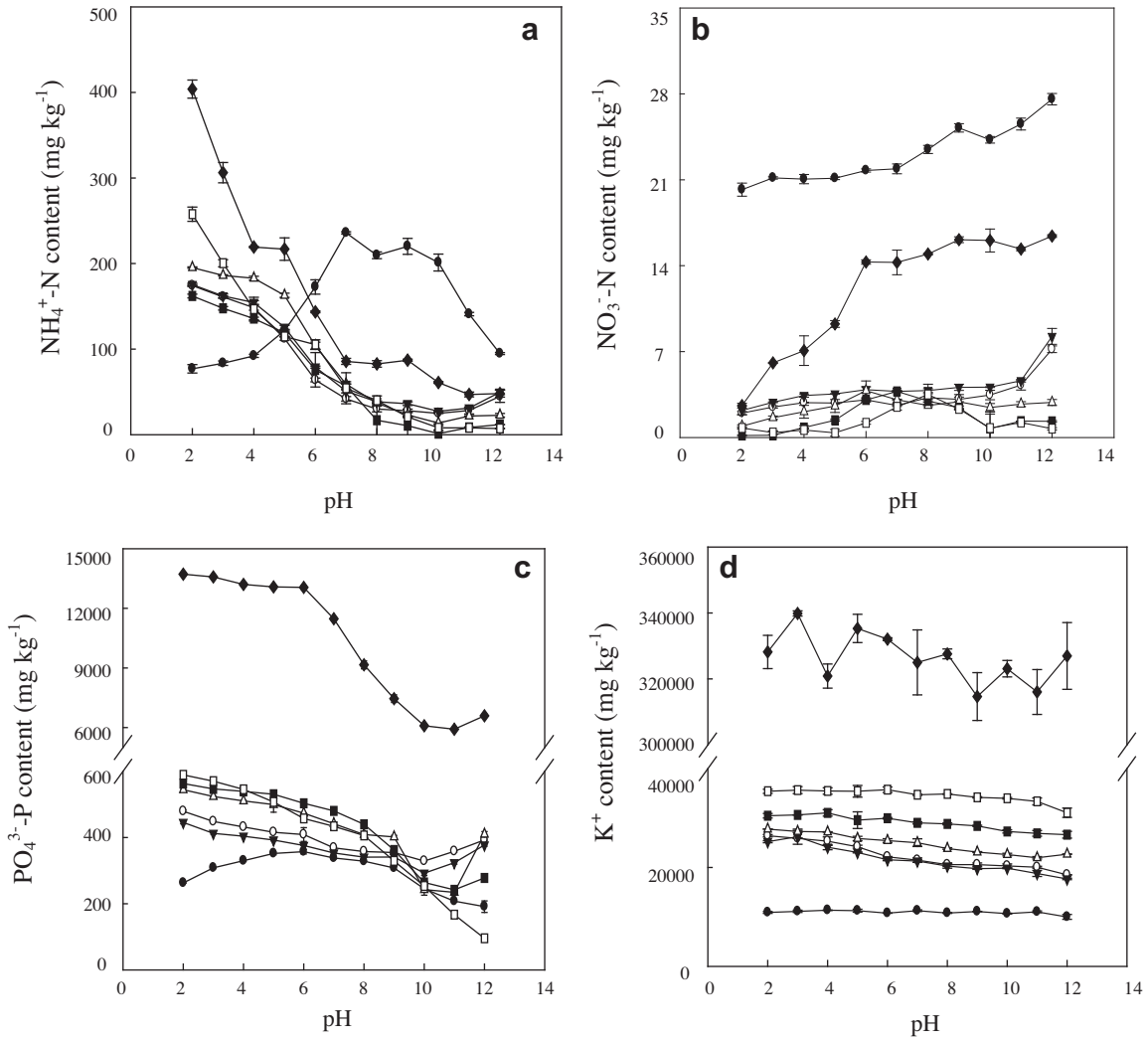

Fig. 3. Nutrient release from biochars at different pH: (a) NH_4^+; (b) NO_3^-; (c) PO_4^{3-}; (d) K^+. Symbols stand for BC0 (●), BC300 (○), BC350 (▼), BC400 (△), BC500 (■), BC600 (□) and BCA (♦). BC0 represents raw giant reed; BC300 through BC600 represent the biochars produced at 300–600 °C; BCA represents the ash sample.

values of NH_4^+ released from biochars using pseudo-first-order model agreed with the experimental q_e (q_e/exp) values more than those from the pseudo-second-order model, while q_e values of PO_4^{3-} and K^+ from the pseudo-second-order model agreed with experimental q_e values (Table 2, Figs. S13–15). The correlation coefficients (R^2) for power function were all above 0.99 for NH_4^+, above 0.98 for K^+ and above 0.95 for PO_4^{3-}, and the kinetic data plots also had a good fit (Table 2, Figs. S13–15). The significant model fits indicates that the power function model can be a good choice for describing the release kinetics of nutrients from biochars. The two parameters of the power function can be viewed as indicators of the initial concentration of nutrients release (a) and the rate at which nutrients release declines with time (b) (Sparks, 2003). Generally, for NH_4^+ and PO_4^{3-}, the parameter a decreased, while b increased with increasing temperatures, indicating lower amounts of NH_4^+ and PO_4^{3-} were released from high-temperature biochars (BC500 and BC600); for K^+, the parameter a increased, while b decreased with temperatures, suggesting that greater amounts of K^+ were released from high-temperature biochars.

3.4. N, P and K release from biochars at different pHs

The pH of the soil or aqueous solution is another important factor affecting nutrient availability of biochars (Silber et al., 2010). The release of PO_4^{3-} and NH_4^+ were pH-dependent, while that of K^+ and NO_3^- was not (Fig. 3). Generally, the content of PO_4^{3-} and NH_4^+ released from the biochars decreased with increasing pH until pH 10, whereas that of K^+ remained relatively stable from pH 2 to 7 and significantly decreased at pH 8–12 (Fig. 3).

The pyrolysis temperature showed different impacts on N, P and K^+ release at a same pH. At pH < 3, BC600 released more NH_4^+ than other biochars, while BC400 released more NH_4^+ at pH 4–6 and BC300 and BC350 released more NH_4^+ above pH 6–12. The amount of NO_3^- released from all the biochars was nearly constant over the whole pH range. The amount of PO_4^{3-} released from high-temperature biochars was larger than that of low-temperature biochars at pH < 8; however, the low-temperature biochars released more PO_4^{3-} at pH > 9. The amount of K^+ released from all biochars increased with increasing temperature over the whole pH range. These results were consistent with the N, P and K content presented in Fig. 1. As discussed earlier, P present in the biochars as amorphous and crystal minerals caused larger amounts of P to be released at lower pH. Consequently, it could be more suitable to use low-temperature biochars (⩽400 °C) to supply NH_4^+ or P in acidic soils, while the biochars may supply sufficient K irrespective of soil pH. What deserves special mention is that biochar may serve as an alkali agent to increase soil pH. Thus, besides supplying the soil with carbon, these biochars can be considered as a promising soil amendment under acidic soil situations (Atkinson et al., 2010; Beesley et al., 2011).

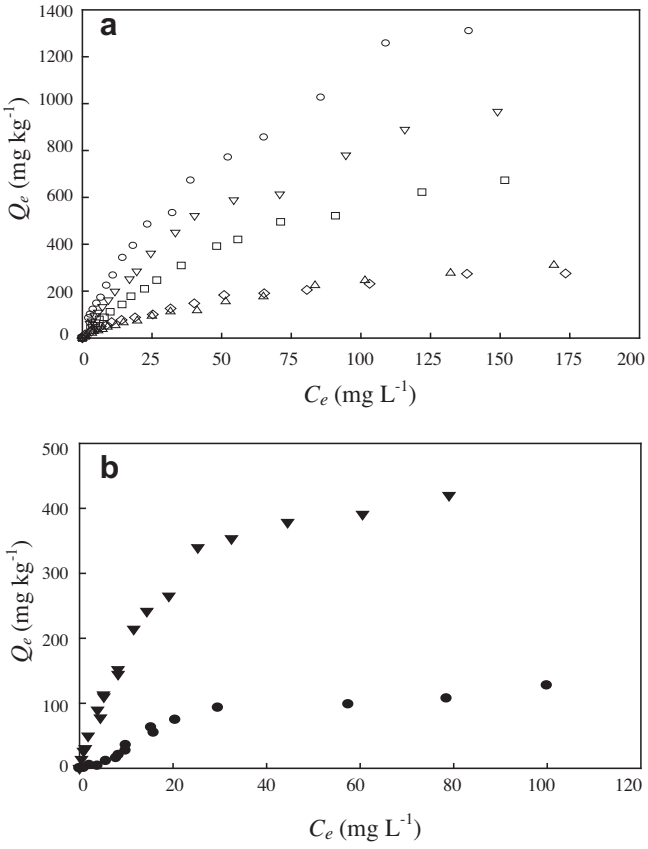

Fig. 4. Sorption isotherms of NH_4^+ (a) and NO_3^- (b) on the biochars at 22 ± 1 °C. (a): Symbols stand for BC300 (○), BC350 (▽), BC400 (□), BC500 (◇), BC600 (△); (b): Symbols stand for BC500 (●) and BC600 (▼). BC300 through BC600 represent the biochars produced at 300–600 °C.

3.5. NH_4^+, NO_3^- and PO_4^{3-} sorption on biochars

Although a certain amount of NH_4^+, PO_4^{3-} and K^+ can be released from biochars, it was reported that biochar may retain nutrients through adsorption (Atkinson et al., 2010). All isotherms of NH_4^+ were nonlinear (Fig. 4a). The Freundlich n values for NH_4^+ remained relatively stable (0.5216 ± 0.0195–0.6524 ± 0.0174) (Table 3). The K_F is a measure of the sorption strength, and the K_F values decreased from 61.08 ± 4.76 ((mg kg^{-1})/(mg L^{-1})^n) for BC300 to 11.49 ± 0.91 ((mg kg^{-1})/(mg L^{-1})^n) for BC600 (Table 3), which indicated that the sorption capacity of NH_4^+ on biochars decreased with increasing temperature. Single-point sorption coefficient (K_1) based on the Freundlich fitting results showed the same order as K_F. In the Langmuir model, the Q^0 values decreased from

Table 3
Regression parameters for the sorption isotherms of NH_4^+ and NO_3^- onto biochars.

Adsorbate	Biochar	Freundlich model				Langmuir model			
		K_F	n	R^2	K_1[α] (L kg^{-1})	K_L (mg L^{-1})	Q^0 (mg kg^{-1})	Q_{chg} (mg kg^{-1} mV^{-1})	R^2
NH_4^+	BC300[β]	61.08 ± 4.76	0.6327 ± 0.0179	0.993	14.52	84.73 ± 7.97	2101.9 ± 107.9	36.19	0.993
	BC350	47.75 ± 4.64	0.6108 ± 0.0221	0.989	10.42	76.37 ± 6.13	1432.6 ± 59.5	24.66	0.994
	BC400	31.76 ± 3.49	0.6210 ± 0.0248	0.987	7.21	83.60 ± 3.72	1043.4 ± 24.7	19.30	0.998
	BC500	20.38 ± 1.77	0.5216 ± 0.0195	0.987	3.14	55.12 ± 5.00	362.8 ± 14.6	7.45	0.990
	BC600	11.49 ± 0.91	0.6524 ± 0.0174	0.994	2.95	58.93 ± 7.88	371.8 ± 22.7	8.00	0.979
NO_3^-	BC500	9.34 ± 2.44	0.5789 ± 0.0662	0.900	1.80	37.51 ± 8.44	171.8 ± 18.6	3.53	0.945
	BC600	56.89 ± 7.57	0.4857 ± 0.0369	0.948	7.61	18.74 ± 1.44	533.5 ± 17.1	11.48	0.992

[α] K_1 is single point adsorption coefficient calculated on the basis of the Freundlich models when C_e was 50 mg L^{-1}.
[β] BC300 through BC600 represent the biochars produced at 300–600 °C.

2102 ± 108 mg for BC300 to 372 ± 23 mg kg^{-1} for BC600 in sorption of NH_4^+, the same trend as that for K_1 derived from the Freundlich model.

NH_4^+ can be easily electrostatically attracted to negative charges on biochar surfaces, since samples in this study carried negative charges at pH 7 (Fig. S5). Thus, the correlation between Q_0 and the surface charge of biochars were analyzed and they showed a negative correlation ($r = 0.929$, $P < 0.05$, Fig. S16a). Also the surface charge-normalized sorption capacity (Q_{chg}) was calculated (Table 3) and the Q_{chg} values had a negative correlation with the pyrolysis temperature ($r = -0.925$, $P < 0.05$, Fig. S16b). The amount of oxygen-containing functional groups had a linear relationship with Q^0 and Q_{chg} (Fig. S16c and d). These parameters indicate that electrostatic attraction is an important mechanism for NH_4^+ adsorption on biochars.

NH_4^+ may be exchanged with Ca^{2+} and Mg^{2+} on the surface of biochars. The amount of water-soluble Ca^{2+} and Mg^{2+} was significantly positively correlated with Q^0 (Fig. S17), indicating that cation exchange may be important for NH_4^+ adsorption on biochars. In addition, BC600 had the highest surface area, but Q^0 was the lowest and the correlation between Q^0 and the surface area of the biochar samples was low (Fig. S18), implying that sequestration in pores was not a dominant mechanism for NH_4^+ adsorption on these biochars.

Interestingly, no significant NO_3^- sorption on low-temperature biochar (BC300, BC350 and BC400) was observed and only a smaller amount of NO_3^- was sorbed by high-temperature biochars (BC500 and BC600). All isotherms of NO_3^- were nonlinear (Fig. 4b) and only the Langmuir model fit the data well (Table 3). The Q^0 was 171 and 533 mg kg^{-1} for BC500 and BC600, respectively, much lower than that reported for wheat straw charcoal and mustard straw charcoal (Q^0 ranged from 1100 to 1300 mg kg^{-1}) (Mishra and Patel, 2009). The lower NO_3^- sorption is related to the NO_3^- species being repelled by negatively charged biochar surface.

No PO_4^{3-} could be sorbed onto BC300 through BC600, owing to the high amount P released from the biochars (Fig. 1c); however, several studies have reported that P can be sorbed by biochars (Chen et al., 2010; Yao et al., 2011). Yao et al. (2011) reported that PO_4^{3-} can be easily removed from aqueous solution through complexation with colloidal and nano-sized MgO particles on the surface of biochars made from digested sugar beet tailings. Additionally, it has been demonstrated that fresh biochar has some anion exchange capacity in the acid pH range, which can initially be in excess of the total cation exchange capacity of the biochar (Cheng et al., 2008). It is possible that these positive exchange sites may sorb PO_4^{3-} through electrostatic attraction. Thus, biochar can also be used as a low-cost waste water treatment technology for PO_4^{3-} removal before its use in soils. In addition, although no PO_4^{3-} was adsorbed onto the GR-derived biochars, organic P in soils may be adsorbed by these biochars due to their high affinity for organic compounds, in turn affecting the P availability in soils.

The low-temperature biochars (⩽400 °C) did not only release more NH_4^+ than that of the high-temperature biochars, but also showed appreciable adsorption capacity for NH_4^+. However, neither PO_4^{3-} nor NO_3^- was adsorbed by these biochars. It should be possible to produce designer biochars with a specific nutrient composition and a specific nutrient sorption property by co-pyrolysis of different feedstocks (Novak et al., 2009). For example, biochar with higher available K and higher sorption capacity for phosphate may be produced from raw GR with MgO minerals or ferrous and ferric chloride at high temperatures (⩾500 °C) (Chen et al., 2010; Yao et al., 2011). Also, blending raw GR with poultry litter as feedstock pyrolyzed at low temperature (⩽400 °C) may result in biochar with higher available P and K, higher liming value and NH_4^+ adsorption than the use of the GR-derived biochar alone in acidic soils (Novak et al., 2009).

4. Conclusions

With increasing temperature of pyrolysis, about 50% of N was lost and remaining N transformed to heterocyclic-N but P and K were not lost. Available P and N in high-temperature biochars decreased. More NH_4^+, PO_4^{3-} and K^+ were released from biochars at low pH (⩽5). More NH_4^+ was adsorbed on the low-temperature biochars (⩽400 °C) than that of high-temperature biochars (⩾500 °C). Thus, taking all factors into consideration, the pyrolysis at or below 400 °C seems optimal for producing biochar from giant reed to improve the availability of N, P and K in soils which are deficient in N, P and/or K.

Acknowledgements

This study was supported by the National Natural Science Foundation of China (41120134004) and USDA Hatch Program (MAS 00982). We are greatly grateful to Dr. Sarah Weis and Dr. Di Zhang for their help with the experiments collecting the data of NH_4^+, NO_3^- and total K.

Appendix A. Supplementary data

Supplementary data associated with this article can be found, in the online version, at http://dx.doi.org/10.1016/j.biortech.2012.12.044.

References

Atkinson, C.J., Fitzgerald, J.D., Hipps, N.A., 2010. Potential mechanisms for achieving agricultural benefits from biochar application to temperate soils: a review. Plant Soil 337, 1–18.
Beesley, L., Moreno-Jiménez, E., Gomez-Eyles, J.L., Harris, E., Robinson, B., Sizmur, T., 2011. A review of biochars' potential role in the remediation, revegetation and restoration of contaminated soils. Environ. Pollut. 159, 3269–3282.
Boehm, H.P., 1994. Some aspects of the surface chemistry of carbon blacks and other carbons. Carbon 32, 759–769.
Bridle, T.R., Pritchard, D., 2004. Energy and nutrient recovery from sewage sludge via pyrolysis. Water Sci. Technol. 50, 169–175.
Cantrell, K.B., Hunt, P.G., Uchimiya, M., Novak, J.M., Ro, K.S., 2012. Impact of pyrolysis temperature and manure source on physicochemical characteristics of biochar. Bioresour. Technol. 107, 419–428.
Cao, X., Harris, W., 2010. Properties of dairy-manure-derived biochar pertinent to its potential use in remediation. Bioresour. Technol. 101, 5222–5228.
Chan, K.Y., Xu, Z., Lehmann, J., Joseph, S., 2009. Biochar: Nutrient Properties and their Enhancement. In: Lehmann, J., Joseph, S. (Eds.), Biochar for Environmental Management: Science and Technology. Earthscan, London, pp. 67–84.
Chen, B., Chen, Z., Lv, S., 2010. A novel magnetic biochar efficiently sorbs organic pollutants and phosphate. Bioresour. Technol. 102, 716–723.
Chen, B., Zhou, D., Zhu, L., 2008. Transitional adsorption and partition of nonpolar and polar aromatic contaminants by biochars of pine needles with different pyrolytic temperatures. Environ. Sci. Technol. 42, 5137–5143.
Cheng, C.-H., Lehmann, J., Engelhard, M.H., 2008. Natural oxidation of black carbon in soils: changes in molecular form and surface charge along a climosequence. Geochim. Cosmochim. Acta 72, 1598–1610.
DeLuca, T.H., MacKenzie, M.D., Gundale, M.J., 2009. Biochar Effects on Soil Nutrient Transformations. In: Lehmann, J., Joseph, S. (Eds.), Biochar for Environmental Management: Science and Technology. Earthscan, London, pp. 251–270.
Etiégni, L., Campbell, A.G., 1991. Physical and chemical characteristics of wood ash. Bioresour. Technol. 37, 173–178.
Gundale, M.J., DeLuca, T.H., 2006. Temperature and source material influence ecological attributes of ponderosa pine and Douglas-fir charcoal. For. Ecol. Manage. 231, 86–93.
Kasozi, G., Zimmerman, A., Nkedi-Kizza, P., Gao, B., 2010. Catechol and humic acid sorption onto a range of laboratory-produced black carbons (biochars). Environ. Sci. Technol. 44, 6189–6195.
Keiluweit, M., Nico, P.S., Johnson, M.G., Kleber, M., 2010. Dynamic molecular structure of plant biomass-derived black carbon (biochar). Environ. Sci. Technol. 44, 1247–1253.
Koutcheiko, S., Monreal, C.M., Kodama, H., McCracken, T., Kotlyar, L., 2007. Preparation and characterization of activated carbon derived from the thermo-chemical conversion of chicken manure. Bioresour. Technol. 98, 2459–2464.

Lang, T., Jensen, A.D., Jensen, P.A., 2005. Retention of organic elements during solid fuel pyrolysis with emphasis on the peculiar behavior of nitrogen. Energy Fuels 19, 1631–1643.

Lehmann, J., Joseph, S., 2009. Biochar for environmental management: science and technology. Earthscan, London.

Mishra, P.C., Patel, R.K., 2009. Use of agricultural waste for the removal of nitrate-nitrogen from aqueous medium. J. Environ. Manage. 90, 519–522.

Novak, J.M., Busscher, W.J., Watts, D.W., Laird, D.A., Ahmedna, M.A., Niandou, M.A.S., 2010. Short-term CO_2 mineralization after additions of biochar and switchgrass to a Typic Kandiudult. Geoderma 154, 281–288.

Novak, J.M., Lima, I., Xing, B., Gaskin, J.W., Steiner, C., Das, K., Ahmedna, M., Rehrah, D., Watts, D.W., Busscher, W.J., 2009. Characterization of designer biochar produced at different temperatures and their effects on a loamy sand. Ann. Environ. Sci. 3, 195–206.

Page, A.L., Miller, R.H., Keeney, D.R., 1982. Methods of Soil Analysis: Chemical and Microbiological Properties, Second ed. American Society of Agronomy Inc., Madison, Wisconsin.

Roberts, K.G., Gloy, B.A., Joseph, S., Scott, N.R., Lehmann, J., 2010. Life cycle assessment of biochar systems: estimating the energetic, economic, and climate change potential. Environ. Sci. Technol. 44, 827–833.

Silber, A., Levkovitch, I., Graber, E.R., 2010. PH-dependent mineral release and surface properties of cornstraw biochar: agronomic implications. Environ. Sci. Technol. 44, 9318–9323.

Sparks, D.L., 2003. Environmental Soil Chemistry, Second ed. Academic Press, Amsterdam.

Spokas, K.A., Cantrell, K.B., Novak, J.M., Archer, D.W., Ippolito, J.A., Collins, H.P., Boateng, A.A., Lima, I.M., Lamb, M.C., McAloon, A.J., Lentz, R.D., Nichols, K.A., 2012. Biochar: a synthesis of its agronomic impact beyond carbon sequestration. J. Environ. Qual. 41, 973–989.

Spokas, K.A., Koskinen, W.C., Baker, J.M., Reicosky, D.C., 2009. Impacts of woodchip biochar additions on greenhouse gas production and sorption/degradation of two herbicides in a Minnesota soil. Chemosphere 77, 574–581.

Sun, K., Ro, K., Guo, M., Novak, J., Mashayekhi, H., Xing, B., 2011. Sorption of bisphenol A, 17α-ethinyl estradiol and phenanthrene on thermally and hydrothermally produced biochars. Bioresour. Technol. 102, 5757–5763.

Wang, J., Morishita, K., Takarada, T., 2001. High-temperature interactions between coal char and mixtures of calcium oxide, quartz, and kaolinite. Energy Fuels 15, 1145–1152.

Wang, X.L., Xing, B.S., 2007. Sorption of organic contaminants by biopolymer-derived chars. Environ. Sci. Technol. 41, 8342–8348.

Wornat, M.J., Hurt, R.H., Yang, N.Y.C., Headley, T.J., 1995. Structural and compositional transformations of biomass chars during combustion. Combust. Flame 100, 131–143.

Yan, L., Liu, Z., Chen, J., He, S., Wu, D., Kong, H., 2005. Subsurface flow type constructed wetland for purification of eutrophic scenic waters. China Water Wastewater 21, 11–13.

Yao, Y., Gao, B., Inyang, M., Zimmerman, A.R., Cao, X., Pullammanappallil, P., Yang, L., 2011. Removal of phosphate from aqueous solution by biochar derived from anaerobically digested sugar beet tailings. J. Hazard. Mater. 190, 501–507.

Yu, C., Tang, Y., Fang, M., Luo, Z., Cen, K., 2005. Experimental study on alkali emission during rice straw pyrolysis. J. Zhejiang Univ. (Eng. Sci.) 39, 1435–1444.

Yuan, J., Xu, R., Zhang, H., 2011. The forms of alkalis in the biochar produced from crop residues at different temperatures. Bioresour. Technol. 102, 3488–3497.